Surface Science 664 (2017) 101–109

Contents lists available at ScienceDirect

Surface Science

journal homepage: www.elsevier.com/locate/susc

Adsorption and thermal stability of 1,4 benzenedimethanethiol on InP(110)

Leonardo Salazar Alarcón[a], Lucila J. Cristina[a,1], Juanjuan Jia[b], Lin Chen[c], Angelo Giglia[d], Luca Pasquali[d,e,f], Esteban A. Sánchez[a], Vladimir A. Esaulov[b], Oscar Grizzi[a,*]

[a] Centro Atómico Bariloche-CNEA, Instituto Balseiro-UNC, CONICET, 8400 S.C. de Bariloche, Río Negro, Argentina
[b] Université de Paris Sud, Institut des Sciences Moléculaires d'Orsay, UMR 8214 CNRS - Université Paris Sud, Université Paris Saclay, Bâtiment 351, Orsay 91405, France
[c] School of Nuclear Science and Technology, Lanzhou University, Lanzhou 730000, China
[d] CNR-IOM, s.s.14, km 163.5 in Area Science Park, Trieste 34012, Italy
[e] Dipartimento di Ingegneria E. Ferrari, Universitá di Modena e Reggio Emilia, Via Vignolese 905, Modena 41125, Italy
[f] Department of Physics, University of Johannesburg, PO Box 524, Auckland Park 2006, South Africa

ARTICLE INFO

Keywords:
Self-assembly
Benzenedimethanethiol films
InP(110)

ABSTRACT

Self-assembly of dithiol molecules is of interest because these can be used as linkers between metallic or semiconductor entities and thus employed in molecular electronics and plasmonic applications, or for building complex heterostructures. Here we focus on dithiol self-assembly by evaporation in vacuum, a method that could circumvent the dithiol oxidation that can occur in solution. We present a high resolution X-ray photoelectron spectroscopy (XPS) and an ion scattering study of adsorption and desorption of 1,4-benzenedimethanethiol on InP(110) as a function of exposure and sample temperature. Results for InP are compared to those on Au(111) and found to differ due to formation of a thick BDMT layer at room temperature, resulting from extra molecules sticking on top of the self-assembled monolayer. This may play an adverse effect in some afore-mentioned applications as in molecular electronics. We furthermore study the evolution of the dithiol film with sample temperature and the elements remaining at the surface after annealing and delineate initial coverage dependent effects.

1. Introduction

The adsorption, self-assembly and thermal stability of thiol-based molecules adsorbed on compound semiconductors such as GaAs and InP has been the subject of considerable research [1–20] due to interest in molecular electronic devices, the passivation properties of the layer, the possibility of obtaining improved optical properties, making Si-InP contacts, microcontact printing, and ultrathin electron beam resists. Amongst thiols, dithiol molecules have attracted interest since the two thiol ends can be bound to metal electrodes and in particular 1–4 benzenedimethanethiol (BDMT) was first used in conduction measurements [21]. They have also been used [5–7, 22–36] for grafting to metallic nanoparticles in plasmonic applications and in building metal-molecule heterostructures [22, 31–35] and metallized graphene like carbon sheets [22, 36].

Self-assembled monolayers (SAMs) of thiol molecules [37–46] are well ordered on several surfaces, but the case of dithiol SAMs is more complicated because the two sulfur ends of the molecules may both bind to the substrate [47, 48] and may not take the more useful upright orientation [22]. In some cases they are also found to link with other molecules producing "multilayers". Multilayer formation in solution has been associated with the oxidation of the thiol group which causes formation of intramolecular disulfide bonds [47–51]. In recent studies we showed that well-ordered standing up SAMs of dithiols could be formed on Au directly in hexane solutions [52–55] that were degassed with inert gases (N_2) and with all the preparation procedure performed in absence of ambient light. In other works acetyl protection and deprotection of the thiol groups has been used [48, 56] or else post assembly removal of S–S bonded multilayers adopted by using reducing agents [27, 57]. The growth of SAMs under vacuum conditions using evaporative methods [26, 30, 58–61] comes as a good alternative to reduce the presence of oxygen and some effects of solvents, particularly in the case of more reactive surfaces such as semiconductors. In the past, we have studied the adsorption in vacuum of BDMT on InP(110) and on Au(111) with Time-of-Flight Direct Recoil Spectroscopy (TOF-DRS) [9] and from the comparison of both systems we were able to show that it was possible to obtain a S terminated layer in the case of the semiconductor. While the presence of sulfur at the organic layer - ambient interface was clearly demonstrated, the structure of this layer was not fully characterized. In particular, in ref [9] we noted differences in the shape of the TOF-DRS

* Corresponding author.
E-mail address: grizzi@cab.cnea.gov.ar (O. Grizzi).
[1] Present address: Instituto de Física del Litoral (IFIS Litoral) - CONICET-UNL. Gral. Güemes 3450, S3000GLN Santa Fe, Argentina.

http://dx.doi.org/10.1016/j.susc.2017.06.003
Received 29 March 2017; Received in revised form 31 May 2017; Accepted 3 June 2017
Available online 5 June 2017
0039-6028/

spectra measured for Au and for InP which indicated variations in the molecule adsorption configuration or the film characteristics that could not be clarified with the limited information available at that moment. More recently we investigated the growth of BDMT on Ag, Au and Cu from vapour phase keeping the sample below room temperature during exposures [62]. For this case we found a strong increase in the sticking coefficient and that the films were thick, i.e. more than one monolayer could be deposited on the three samples. In all cases the thick BDMT layer desorbed around 270 K leaving a thin BDMT monolayer at the surface.

In this work we performed a high resolution X-ray photoelectron spectroscopy (XPS) study of the BDMT layer grown on InP(110) together with additional TOF-DRS measurements as a function of exposure and on sample temperature, to probe in more detail the structure and stability of the BDMT layer. TOF-DRS measurements on Au(111) as a function of both exposure and temperature are also reported to clarify the discussion and to extend the results for the annealing temperature dependence initiated in ref [62]. An XPS study of BDMT evaporated on Au(111) was presented recently [63]. Based on these new measurements and the previous information for metallic substrates we show that part of the differences observed in InP with respect to the Au substrate are due to formation of a thicker BDMT layer for adsorptions carried out at room temperature, with extra molecules attached at the SAM-ambient interface. The thickness of this layer is discussed in the text.

2. Material and methods

The TOF-DRS measurements were performed using an ion scattering system described in some detail elsewhere [64], while the XPS measurements were performed on the BEAR beamline [65] at the Elettra synchrotron (Trieste, Italy). Some details for each system are provided below.

2.1. Ion scattering

The ion scattering system has facilities for in situ sample preparation and characterization under UHV conditions. The system is connected to a mass selected 1–100 keV ion accelerator. The experiments are performed using the time of flight direct recoiling technique (TOF-DRS) [66]. In TOF-DRS, the sample is bombarded by a pulsed beam of 3–6 keV Ar^+ ions at different incidence angles, here reported with respect to the surface plane. A time-of-flight analysis of the primary recoiled (DR) target atoms and of the scattered Ar atoms is performed by using a channel electron multiplier placed at the end of a 1.76 m long time-of-flight tube set at a forward angle of 45° with respect to the incidence beam direction. As described in ref. [66] TOF-DRS has a very high sensitivity to the top-most layer of a crystalline surface. The emission of target atoms in primary collisions with the projectile, both from the substrate (Au, In, P) or from the adsorbed layer (H, C, S), here reported as “recoil particles Au, In, C, etc.”, provides information about the elemental composition. The strong shadowing and focusing effects [66] in these processes help to delineate if the molecules are adsorbed with both S atoms towards the surface or in a more standing-up orientation exposing one S atom to the vacuum interface [62, 64]. The process of projectile scattering from a given target atom in a primary collision (here indicated as Ar - R, with R: Au, In, or S) is more sensitive to sub-surface processes and is useful to identify if the layer adsorbed is thin (one monolayer or less) or thick (more than two monolayers) [62].

In TOF-DRS the low intensity pulsed beam minimizes damage, which is important in the case of organic layers. One can thus follow in detail the adsorption and desorption kinetics from submonolayer to very high exposures without damaging the film and also obtain information on the layer composition as a function of sample temperature. The absence of damage is checked by taking several spectra after a given exposure and verifying that there are no visible changes.

2.2. XPS studies

XPS spectra were acquired with a hemispherical deflection analyser, with an energy resolution of <200 meV (analyser and beam line, using a constant pass energy). Spectra were recorded at normal emission, with the light impinging at 45° with respect to the surface normal. Spectra were acquired in the P 2p, In 3d and 4d, S 2p, O 1s and C 1s regions. We also measured the valence band for photon energies between 120 and 60 eV. We strove to use photon energies that maximize the surface sensitivity, measuring photoelectrons with kinetic energies corresponding to the minimum of the inelastic mean free path (100 eV), though in some cases some other energies are chosen for convenience, in particular to avoid overlap with Auger peaks.

2.3. Sample preparation

The InP(110) single crystals were prepared by cycles of Ar sputtering with energies of 0.5–1 keV and annealing at 700 K, and then characterized with respect to cleanliness and surface order by TOF-DRS and by XPS following earlier studies [67–70].

The BDMT powder (from Sigma Aldrich, 98% purity), was kept in vacuum, in a sealed glass tube. It was degassed and heated to about 360 K and the vapours were introduced into the UHV chamber via a leak valve. On the BEAR beamline the exposure to the vapours was performed in a load lock chamber to avoid contamination of the main UHV system.

3. Results and discussion

3.1. Clean sample

It is known from earlier works on InP [67, 68] that sputter cleaning InP surfaces can induce defects and produce an In enriched surface. This results in changes in the In 4d and in the P 2p spectra, but it was pointed out that these effects could be much reduced after annealing. The analysis of our high resolution XPS measurements in the In 4d and in the P 2p regions of samples cleaned using fairly low energy ion sputtering and annealing to temperatures in the 700 K range produced reasonably good results with only a small fraction of In enrichment. Valence band spectra acquired for different photon energies clearly indicate the existence of a circa 1 eV gap, which is usually observed for UHV cleaved InP samples. Details of these measurements are described in the supporting information and presented there in Fig. S1. On the basis of all these results we concluded that the InP surfaces thus produced were adequate for the study of BDMT adsorption.

Prior to performing the BDMT adsorption an ion scattering study of the cleaned InP surface was also performed and details are summarized in the supporting information and Fig S2. Ion scattering spectra in the forward direction are sensitive to both the crystallographic characteristics of the sample and its elemental composition. The preliminary study of the clean surface along various azimuthal directions allowed us to determine the orientation of the sample and all the measurements shown below for the adsorption and desorption studies were taken along a direction where both In and P are accessible to the projectile at an incident angle of 20°.

3.2. Adsorption of BDMT on InP(110): comparison with BDMT on Au(111)

3.2.1. Adsorption monitored by ion scattering

As mentioned in the introduction we performed a previous ion scattering study of BDMT adsorption onto InP(110) [9] and were able to show that it was possible to discriminate between BDMT layers dominated by a lying down molecule configuration at low exposures, below few kL or by a standing up configuration at high exposures (above 5×10^4 L): a layer that was terminated by sulfur. A comparison with results for Au(111) [9, 60, 61] showed that the width and the relative

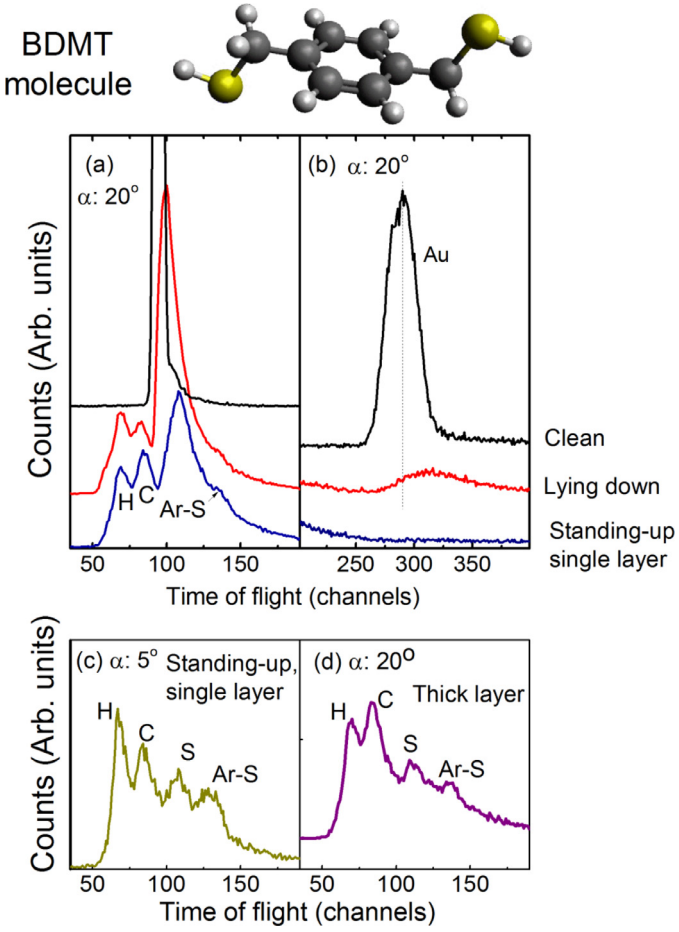

Fig. 1. TOF-DRS spectra for BDMT adsorbed on Au(111) at 250 K for different stages of the BDMT layer growth. (a) spectra in the TOF region of H and C recoils, and Ar scattering, taken at 20° incidence for the clean surface (top), for a thin BDMT layer with molecules in a predominantly lying-down configuration (middle), and for a single layer of standing-up molecules (SAM) (bottom). (b) same as (a) in the TOF region of Au recoils. (c) spectrum for the SAM (single layer) taken at 5° incidence. (d) spectrum at 20° for a multilayer of BDMT on Au(111) taken at 20° incidence.

intensity of the H, C recoil peaks and the Ar scattering peaks were different indicating a different evolution of the layer growth on Au and on InP with exposure or a different molecular arrangement. Here we address this point with the aid of XPS and with additional ion scattering measurements. We start by describing the ion scattering measurements. First we present and discuss some data for Au because it serves as reference of a known system.

3.2.1.1. BDMT on Au(111). Fig. 1 shows ion scattering spectra measured at specific phases of the BDMT layer growth on Au(111). Following ref [62] and in contradistinction with most works done up to date the sample temperature was lowered to 250 K during exposure. Panels a and b in Fig. 1 show spectra for the clean surface (top spectrum), after formation of the initial lying down layer, and after completion of the first standing-up layer. The left panel (a) shows the spectra in the TOF regions corresponding to H, C and S and the right panel (b) the region for the Au recoil peak. The spectra were acquired at an incident angle of 20°. Similarly to what was reported for Ag(111), here the main changes in the spectra with BDMT exposure are the appearance of the H and C recoil peaks, a decrease, shift and broadening of the Ar scattering peak, and a strong reduction of the substrate (Au) recoil peak. Each phase is characterized by specific features, for example in the initial phase, i.e., in the lying down phase:

(a) the H peak is bigger than the C peak,
(b) the features associated with S are hardly seen because (i) both S atoms of the molecule are lying closer to the substrate and shadowed by the rest of the molecule (see molecule scheme in Fig. 1) and (ii) the peak due to Ar scattering-off Au appears in the same TOF region and is very intense. Finally,
(c) the Au recoil peak observed at 20° incidence decreases approximately by a factor of 10 and shifts to higher TOFs (Fig. 1(b)). This shift of the Au peak, not observed for Ag in ref [62] is related to the migration of some Au atoms into the organic layer. This would confirm conclusions of other works that Au adatoms are present in the SAM-Au interface [39]. The latter point is discussed further in the supporting information.

Following Fig. 1, the standing-up phase in Au is characterized by:

(a) a change in the ratio of H to C recoil peaks, the C peak becomes bigger than the H peak,
(b) a stronger reduction of the Ar scattering peak (bottom spectrum, Fig 1(a),
(c) the complete disappearance of the Ar scattering peak at more grazing incidence (5°) together with the appearance of the S associated peaks (S recoil and Ar–S scattering, Fig. 1(c).

This appearance of the S peaks at grazing incidence is the fingerprint of a layer terminated in S (S atoms exposed to vacuum) [9, 62]. When the exposure to BDMT is carried out with the sample at room temperature, the above described features correspond to the saturation condition, i.e., extended exposures, increasing both thiol pressure and/or exposure time produce no more changes in the TOF spectra, meaning that the layer thus formed is very thin, saturated with one monolayer of standing-up molecules [9, 62]. On the other hand, when the exposures are carried out with the sample at temperatures below or around 250 K the adsorption kinetics changes [62], resulting in a strong increase of the sticking coefficient, and upon increasing the exposure time and the dithiol pressure it is possible to form a thicker BDMT layer (more than 2–3 layers). In this case the spectra at large angles and those at grazing angles become similar because the Ar projectiles cannot reach the Au substrate, then, only peaks due to H, C and S are seen, without any effect induced by the underlying substrate (complete disappearance of Au associated peaks for all incident angles) [62]. The spectrum corresponding to this condition (thick BDMT layer, acquired at 250 K) is shown in Fig. 1(d). This layer desorbs in the range of 265–270 K, leaving a single layer of BDMT on the surface [62]. As shown in ref. [62] each of the described phases are formed at very different exposures, ranging from less than 1 to 10^4 L when the adsorptions are carried out at 250 K, and from several L to $>10^6$ L at RT. To cover this broad range of exposures in reasonable laboratory times one is forced to change both thiol pressure and exposition time. Now, with the knowledge of the scattering features for the different adsorption phases on Au we proceed to describe the adsorption on InP(110).

3.2.1.2. BDMT on InP(110). Spectra measured at large (20°) and low (5°) incident angles for different exposures to BDMT, keeping the InP(110) surface at room temperature (RT) are shown in Fig. 2(a)–(c). The azimuth was chosen such that at 20° incidence both In and P are clearly seen, while at 5° the features related to P are enhanced by focusing so any change on them can be seen clearly. Comparing with the Au(111) case we find a number of similarities, common to BDMT adsorption on other surfaces, but also some important differences. As for Au, the adsorption goes through different stages, here corresponding roughly to exposures below 10^2 L, from 10^2 L to about 10^4 L, from 10^4 to 10^5 and above. In the initial region of exposures (up to around 100 L) the molecules are oriented preferentially in a lying down configuration, with the majority of the S atoms not exposed to the vacuum interface. This is evidenced by an initial drop of the P associated features, of the In DR peak (without disappearing completely), and the corresponding increase in the H and C peaks that grow very rapidly and reach a relatively stable condition around 10^2 L. The substrate DR peaks decreases

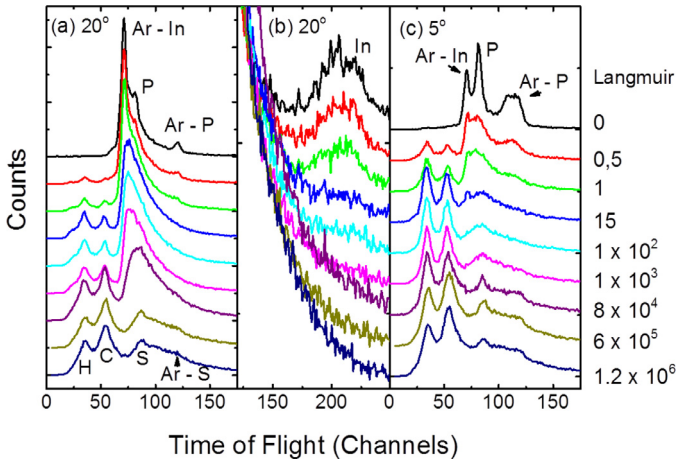

Fig. 2. TOF-DRS spectra for BDMT adsorbed on InP(110) at different exposures for two different incident angles. (a) spectra at 20° incidence in the TOF region for H, C, P and S recoils plus Ar scattering from both substrate and S, (b) same as (a) in the TOF region for In recoils, and (c) same as (a) taken at 5° incidence. The BDMT exposures in Langmuir are indicated on the right side of the figure. The same colours are used in the different panels for equal exposures.

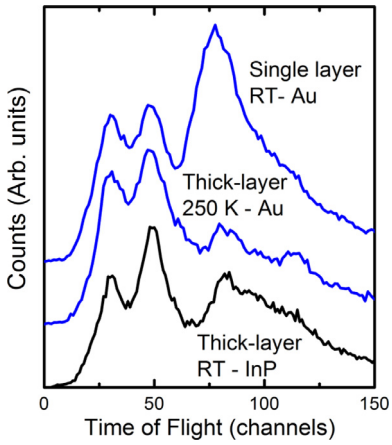

Fig. 3. Comparison of TOF-DRS spectra for InP(110) at RT with those for Au(111) at RT and at 250 K. All spectra were acquired after saturation with BDMT.

without shifting from its initial position. This means that there is no major change in the substrate order and saturation of the lying-down regime occurs with a layer that allows some In atoms to be exposed to the incident beam. Some changes in the spectra take place even in this regime, the width of the H and C DR peaks increase continuously as well as their intensity ratio. This implies that some reordering or change takes place in the organic layer without reaching a perfectly stable lying-down phase, as is the case for BDMT / Ag(111). The next stage, for exposures up to 10^4 L, is characterized by a lower sticking coefficient, an increase of the C/H ratio, and the persistence of the Ar scattering from the InP substrate at high incidence angles. S associated features (recoil and Ar scattering) begin to be observed at grazing angles, but not at large incidence angles. The spectra in this stage are thus compatible with a thin layer of mixed phases composed of lying-down and standing-up molecules.

With increasing exposures, the molecules undergo the transition to standing-up, evidenced by well-defined S associated peaks at grazing incidence, and the complete disappearance of the In recoil peak. The layer remains thin (on the average), of the order of the monolayer up to 10^5 L, when another decrease in the Ar scattering from substrate atoms starts to be observed at 20°. Finally, higher exposures to BDMT result in further changes in the TOF spectra, now the grazing and the large incidence spectra become very similar (bottom spectra in Fig. 2(a) and (c), which means that the layer increased the thickness and thus precluded the access or scattering from the substrate. Here, only features related to the molecule (S, H and C) can be seen. According to the simulations of ref [9] the layer formed has to be thicker than 2–3 monolayers, otherwise some contribution from the substrate as multiple scattering would be seen. Note that while in Au this condition is only obtained at sample temperatures of 250 K or lower, in InP this condition is reached at room temperature. The comparison of these saturation conditions for both surfaces is shown in Fig. 3. These results are relevant because often one tends to expose the surface to large doses of dithiol vapour to obtain a better order in the organic layer or a more complete coverage, this may result adequate in the case of Au however it will certainly generate a thicker layer (and probably more disordered) in the case of InP. The formation of a thick BDMT layer at RT in InP(110) is thus different to the case of dodecanethiols on the same surface, where the formation of a single domain monolayer has been described in detail [4], these new results are discussed further below based on the XPS measurements.

3.2.2. *Adsorption monitored by XPS*

In order to get more insight into the nature of the BDMT layer we performed some measurements at intermediate (4000 L) and high (400 kL) exposures of the InP(110) surface to BDMT; the former corresponding to the transition from lying-down to standing-up, and the latter now assigned to formation of a thick layer as discussed above. These results are summarized in Fig. 4(a)–(c).

Before discussing these spectra a few words about the S 2p core level binding energies in thiol and dithiol self-assembly are necessary, since the spectra can be quite complicated and consist of several components [22, 63]. In the following we cite the energies of the lowest energy S $2p_{3/2}$ doublet component, which have been generally found to appear at about 161, 162, 163.1 eV, and also between 163.3 and 163.8 eV. These are assigned as follows:

(a) Previous works on thiol SAMs mainly on metal surfaces and also on GaAs [22, 37, 38, 43, 52–55, 71, 72] show that the S 2p peak corresponding to thiolate S (S bound to the substrate) lies at about 162 eV. This is also the case for the lying down phase of dithiols with both S ends tethered to the metal as shown for dithiols like BDMT adsorption on coinage metals (Au, Ag and Cu) [55, 63, 71].

(b) In well-ordered BDMT SAMs with standing up molecules [52–54] there appears a strong peak at about 163.1 eV related to the outer SH group.

(c) In some cases of thiols and also BDMT adsorption [44, 54, 55, 63] one observes a smaller structure at about 161 eV attributable to an alternative adsorption site of thiolate S. Note that this has sometimes been assigned to atomic S from dissociation or beam damage, but the peak sometimes appears in a transitory manner [44], which does not favour attribution to strongly bound atomic S and it also does not appear after intense irradiation of aromatic thiols [73, 74]. On the other hand atomic S does appear in spontaneous S–C bond scission on a reactive surface as this is observed in BDMT adsorption on Cu [71].

(d) The higher lying components have been attributed to S–S bonded molecules and S in “free” thiols. The 163.6 eV peak has been observed in poorly rinsed thiol SAM preparation in solution and attributed to extra thiols sticking on top of the SAM [43, 63]. It is also seen in thiol and BDMT films on graphite and in very high exposures of BDMT on Ag and Cu [63]. Finally there also exists the possibility of creation of S–S bonded molecules by irradiation [73] and this has been observed in alkanethiol irradiation but not for aromatic thiols. This assignment is based on a comparison with films of disulfide (RS–SR) molecules. These attributions are supported by DFT calculations [63]. Keeping this in mind we now turn to the spectra from BDMT on InP.

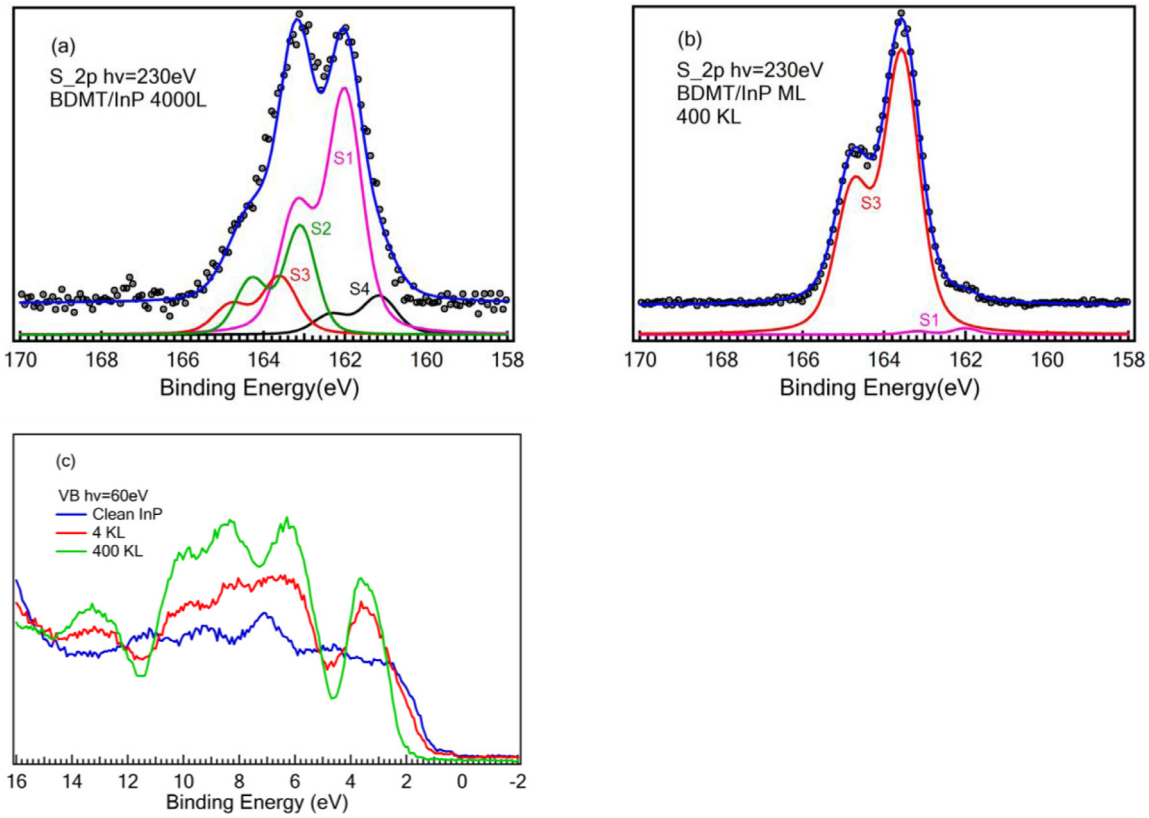

Fig. 4. XPS spectra in the S2p (a) and (b), and valence band regions (c) for BDMT on InP for low and high exposures. The clean InP valence band spectrum is also shown in pannel (c). lines in panels (a) and (b) are fits described in the text. The experimental spectrum and the sum of the different fitting components are displaced vertically for clarity.

XPS spectra in the S2p region are shown in Fig. 4 after a 4000 L and a much higher dose of 400 kL. After a Shirley background subtraction the spectra were fitted with several doublets corresponding to the S $2p_{3/2-1/2}$ components with a 1.2 eV spin orbit splitting and a branching ratio of 0.5, using a Voigt contour. The lower exposure spectrum (Fig. 4a) displays two main peaks at about 162 eV and about 163 eV. In the fit we use two main components with S $2p_{3/2}$ at 162 eV corresponding to thiolate S bound to InP (indicated as S1 in Fig. 4(a)) and a second smaller S $2p_{3/2}$ peak at about 163.1 eV (S2), which we ascribe to "free" S corresponding to the SH end of a standing up molecule [63]. To properly fit the spectra we include two smaller components lying at about 161 eV (S4) and 163.6 eV (S3). The dominance of the 162 eV component (S1) indicates that we have predominantly lying down BDMT molecules with both S ends bound to the substrate.

In thiol adsorption one assumes that a deprotonated –SH end of the BDMT is bound to the surface. Earlier studies of thiol adsorption on InP conclude that S is bound to In, whereas H can be bound to P or liberated.

When the BDMT dose is much higher the S 2p spectrum changes dramatically and is dominated by the 163.6 eV peak (S3, Fig. 4(b)). The 162 eV peak is now barely visible (S1). Its area with respect to the main peak is <5% of the main peak. This spectrum must correspond to a thick layer of BDMT, with extra BDMT molecules sticking or physisorbed to the surface of the BDMT monolayer as discussed above. Assuming as in our earlier study of BDMT adsorption on Au [54] that for 100 eV kinetic energy electrons the attenuation length is about 0.6 nm, one can say that the effective thickness of the layer is more than 2 nm (i.e. more than about 3 BDMT layers), considering the layer to be homogeneous. This thick layer explains the similarity in the ion scattering spectra at low and high incidence angles for high exposures. Similar effects of multilayer formation were observed in our earlier studies dealing with BDMT evaporative adsorption on Ag and Cu [71], where large exposures lead to what we interpret as being a SAM of standing up BDMT molecules on top of which there is a considerable amount of physisorbed BDMT.

Finally, Fig. 4(c) shows changes in the valence band region upon BDMT adsorption. One observes a progressive decrease of the InP related features between 1 and 2 eV and at higher energies appearance of BDMT related structure at 3 eV. At the high dose the spectrum is dominated by BDMT [54], in agreement to the thick layer deduced from the S 2p XPS spectrum and thus further supports our conclusion that we do get a multilayer in these conditions.

An interesting general question is why a fairly stable thick layer of BDMT forms on InP in vacuum. Similar effects were noted in some cases for Au(110), Ag and Cu substrates [71] in vacuum evaporation of BDMT. A tentative explanation could be that if the initially formed SAMs with standing-up dithiols are poorly organized, then additional molecules arriving at very large exposure could be entangled or trapped within the SAM and the thus produced disordered layer mediates further trapping of molecules. The fact that the vacuum evaporated dithiol SAMs differ from those produced in liquid phase adsorption follows from appearance of additional "alternative" adsorption sites with different core level binding energies [54, 71].

3.3. Desorption of BDMT

Self-assembled monolayers of long chain alkanethiols on InP were found to be more passivating towards oxidation than S alone [16]. However this passivating behaviour seems to change at elevated temperatures (above 473 K) due to film degradation [16]. It becomes interesting then to study the surface composition versus temperature for thiol-based molecules. Here we use ion scattering to follow the evolution with temperature of all elements of the BDMT molecule adsorbed on InP(110) and compare it to BDMT on Au(111). These ion scattering measurements are complementary to the more standard thermal desorption experiments (TPD, not available in our system) in the sense that they detect the elements remaining at the surface while TPD detects the molecular species leaving the surface.

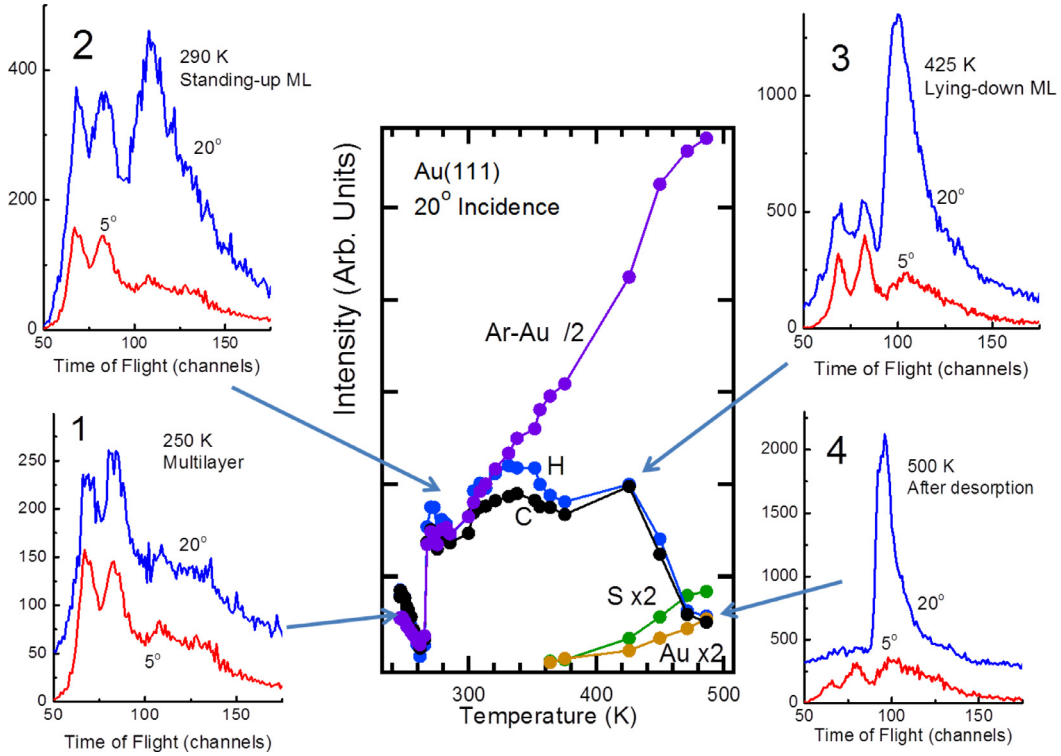

Fig. 5. Central panel: evolution of the intensity of characteristic peaks (H, C, S and Au) in TOF-DRS spectra measured at 20° incidence for a thick BDMT layer on Au(111) versus sample temperature. The insets show typical spectra at both 20° and 5° incidence corresponding to the: multilayer at 250 K (inset 1), standing-up monolayer obtained at 290 K (inset 2), lying-down monolayer after annealing to 425 K (inset 3), final desorption for temperatures of 500 K (inset 4).

As we have done above for the adsorption kinetics of BDMT, we start the discussion with results for BDMT/Au(111) which serves as a reference system. For this purpose we extend the temperature range of the annealings to around 500 K, i.e., well beyond of those described in ref [62] where only the desorption of the multilayer was investigated. Some characteristic spectra at both 20° and 5° incidence, together with the area of the main peaks are shown versus temperatures in Fig. 5. As discussed above, we start from an initial condition corresponding to a thick layer (more than 2–3 layers) formed at 250 K (bottom left, inset 1).

With increasing temperature, still below RT, the intensity of the peaks decrease and they become broader suggesting that the thick layer is disordered or melted (not shown), and around 268 K a sharp layer desorption takes place [62], which is evidenced by a rapid increase and sharpening of the peaks, accompanied by an increase of the pressure in the vacuum chamber. At this condition the surface remains covered by a thin layer (monolayer) which allows the incoming ions to reach the substrate, giving rise to a strong Ar–Au peak. The molecules are predominantly oriented in a standing-up configuration, evidenced by the S associated peaks observed at grazing incidence (left top, inset 2). This stage is approximately stable up to around 350 K, where the S associated peaks in the grazing spectra start to decrease till complete disappearance around 400 K. This transition is accompanied by some molecule desorption evidenced by an increase of the contribution of the substrate peak (Fig. 5, inset 3 right top). Finally, around 430 K the desorption of the lying-down layer starts reaching a final condition around 470–500 K, with some S, C and H remaining at the surface (right bottom, inset 4). This residual layer requires sputtering (coupled with annealings) to be removed. The content of S after desorption is rather independent of the initial condition, i.e., starting from a dilute lying down layer, a dense standing-up monolayer or a thick layer results in approximately the same amount of remaining S. This suggests that this S is generated in the last desorption stage where for some molecules the S–C bond is cleaved. In contradistinction, the C remaining at the surface depends strongly on the initial configuration: there is no C or H left at the surface when the initial condition is the lying-down layer, while some C and H remain for the standing-up layer. The origin of this curious effect is not clear. Possibly in the latter case a stronger initial restructuring of the Au surface upon thiol adsorption allows carbon Au links, related to Au adatoms or atoms at steps (or pits that appear in SAMs) to be formed after S–C bond breaking. C–Au bonding occurs in case of terminal alkyne and acetylenes SAMs on Au [75, 76] This point is further discussed in the supplementary information.

The desorption of BDMT from InP(110) also has well defined stages and depends on the initial condition or coverage. We describe first the desorption from an initial condition with predominance of a single layer without full development of the thick layer. This corresponds to a condition where the S associated peaks are seen at grazing incidence while the contribution to the TOF spectra from the substrate is still important at 20° incidence. The spectra at grazing incidence change as a function of temperature as shown in Fig. 6. The layer is stable up to around 360 K, where desorption begins leading to a transition to a lying down molecule configuration, that is characterized by the disappearance of the Ar–S peak at grazing incidence, and an increase in the substrate contribution. Then, around 500 K a new change occurs where most of the C and H start to go away. It is difficult to be sure about the fate of S because its mass is close to that of P. However the width and position of the peaks after desorption suggests that some S remains at the surface, as is the case for other thiols on GaAs. In previous works [16] on octadecanethiol adsorption on InP it was indeed noted that S remained on InP after heating to 673 K. This indicates S–C bond cleavage at high temperature.

Some differences occur when the initial condition is a thicker layer, where the starting TOF-DRS spectra at grazing and at 20° incidence are similar, without showing contributions from the substrate. In comparison to Au, the thick layer survives well above RT and presents less defined transitions than the monolayer on InP described above. It evolves more smoothly as shown in Fig. 7, where the area of the C peak is com-

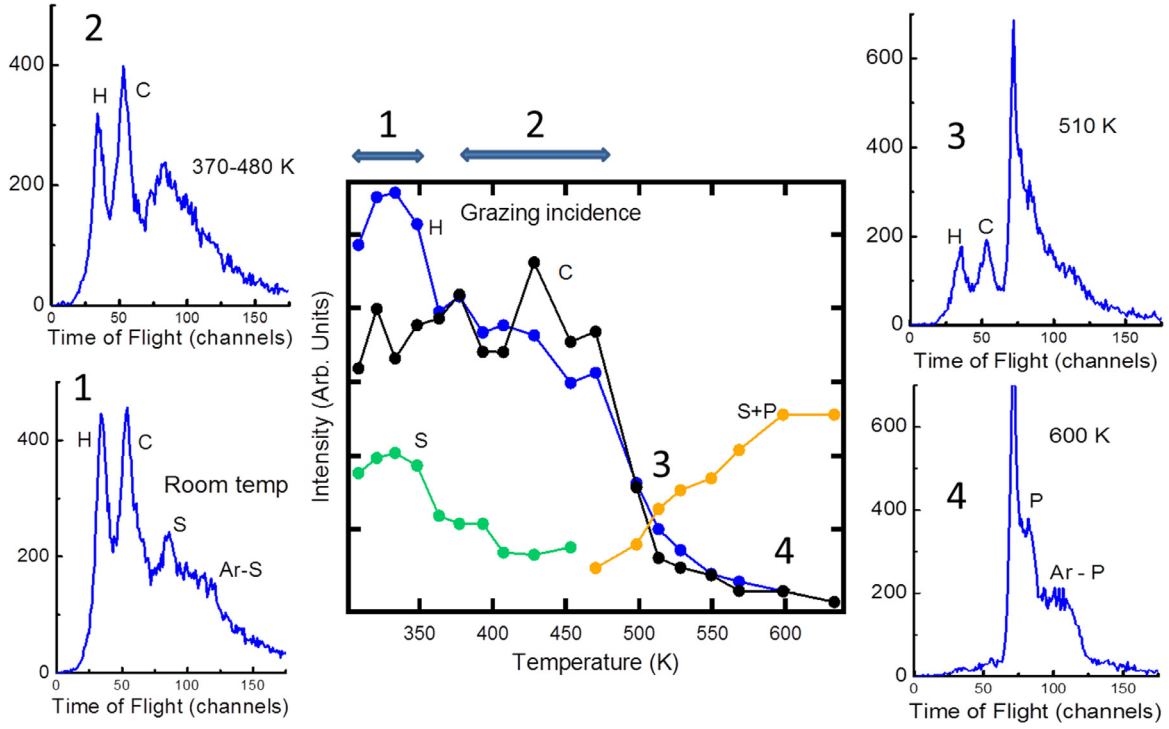

Fig. 6. Central panel: evolution of the intensity of characteristic peaks in TOF-DRS spectra for BDMT adsorbed on InP(110) versus sample temperature starting from an initial condition of a standing-up BDMT layer. Insets 1–4: typical spectra measured at 5° incidence in the temperature ranges indicated in the central panel.

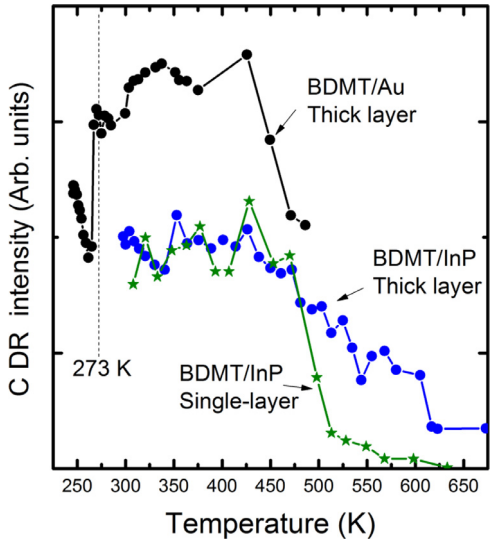

Fig. 7. Comparison of the evolution of C DR intensity versus temperature for single and thick BDMT layers on InP(110) and for a thick layer of BDMT on Au(111).

pared for BDMT on Au and InP (low and high exposures). The main desorption occurs at 40–50 K higher than in Au, evidencing the stronger interaction with the semiconductor.

4. Conclusions

The high resolution XPS and ion scattering experiments on BDMT adsorption from the vapour phase on InP(110) and Au(111) confirm that at low exposures a lying down BDMT phase with both S atoms attached to InP is preferentially formed. At high exposures, close to hundred thousand Langmuir, a mainly standing up phase is formed with S exposed at the SAM vacuum interface. At still higher exposures (beyond several hundred thousand Langmuir) a thick BDMT layer is formed. These adsorption results for InP are different from the Au case at RT where the present and earlier measurements show that the organic layer is dominantly a monolayer on which some molecules may be physisorbed, i.e., a thick layer is not formed at RT, but only at low temperatures of about 250 K. XPS also shows a small component at 161 eV in the initial phases of adsorption on InP that could be attributed to either some atomic S or to some molecules adsorbed on different (alternative) adsorption sites as this was also noted for Au(111).

Upon heating the sample, on both substrates BDMT desorbs, leaving some S atoms following S–C bond scission. Interestingly ion scattering shows that in case of Au, if desorption is performed after the formation of a standing up phase, a substantial amount of H and C remain on the substrate, while this does not occur to a significant extent if the starting condition is a lying down phase. Desorption from InP is observed to occur at somewhat higher temperatures than from Au, suggesting possibly stronger bonding with InP.

From a general point of view appearance of thick layers instead of a standing up monolayer in evaporative adsorption would play an adverse effect in certain applications. Thus, in conduction measurements it would not be clear what is being characterized. This effect was previously not noted [26, 30, 58, 59] but must be taken into account, and eventually minimized by careful tuning of the exposures. A detailed characterization of the type of organic layer formed will thus be essential.

Acknowledgements

J.Jia and L. Chen thank the Chinese Scholarship Council for the fellowship provided to pursue research in France. This work was supported by the CNRS French-Argentina International Laboratory for Nanoscience (LIFAN). The research leading to these results has received funding from the European Community's Seventh Framework Programme (FP7/2007–2013) under grant agreement n° 312284. E.A.S. and O.G. acknowledge partial support from U.N.Cuyo (06/C517) and CONICET (PIP 112-201101-00594 and 112-201501-00274).

Supplementary materials

Supplementary material associated with this article can be found, in the online version, at doi:10.1016/j.susc.2017.06.003.

References

[1] L.C. McGuiness, A. Shaporenko, C.K. Mars, S. Uppili, M. Zharnikov, D.L. Allara, Molecular self-assembly at bare semiconductor surfaces: preparation and characterization of highly organized octadecanethiolate monolayers on GaAs(001), J. Am. Chem. Soc. 128 (2006) 5231–5243.

[2] L.Ch. McGuiness, D. Blasini, P.J. Masejewski, S. Uppili, M.O. Cabarcos, D. Smilgies, L.D. Allara, molecular self-assembly at bare semiconductor surfaces: characterization of a homologous series of nAlkanethiolate monolayers on GaAs(001), ACS Nano 1 (1) (2007) 30–49.

[3] D. Zerulla, T. Chassé, Structure and self-assembly of Alkanethiols on III–V semiconductor (110) surfaces, J. Electron Spectrosc. Relat Phenomena 172 (2009) 78–87.

[4] D. Zerulla, T. Chassé, Scanning tunneling microscopy and spectroscopy of UHV-deposited dodecanthiolate films on InP(110) surfaces at consecutive doses: a single domain system, Langmuir 18 (2002) 5392–5399.

[5] A.D. Krapchetov, H. Ma, K.Y.A. Jen, A.D. Fischer, Y. Loo, Deprotecting thioacetyl-terminated terphenyldithiol for assembly on Gallium Arsenide, Langmuir 24 (2008) 851–856.

[6] A.D. Krapchetov, Ma, K.Y.A. Jen, A.D. Fischer, Y. Loo, Solvent-dependent assembly of Terphenyl- and quaterphenyldithiol on gold and Gallium Arsenide, Langmuir 21 (2005) 5887–5893.

[7] Y. Loo, V.D. Lang, A.J. Rogers, W.P.J. Hsu, Electrical contacts to molecular layers by nanotransfer printing, Nano lett. 3 (7) (2003) 913–917.

[8] L.M. Rodríguez, J.E. Gayone, E.A. Sánchez, O. Grizzi, B. Blum, R.C. Salvarezza, L. Xi, W.M. Lau, gas phase formation of dense alkanethiol layers on GaAs(110), J. Am. Chem. Soc. 129 (2007) 7807–7813.

[9] S.L. Alarcón, L. Chen, A.V. Esaulov, E.J. Gayone, A.E. Sánchez, O. Grizzi, Thiol terminated 1,4-benzenedimethanethiol self-assembled monolayers on Au(111) and InP(110) from vapor phase, J. Phys. Chem. C 114 (47) (2010) 19993–19999.

[10] Ch. Zhou, C.J. Jones, A. Trionfi, W.P.J. Hsu, V.A. Walker, Electron beam-induced damage of alkanethiolate self-assembled monolayers adsorbed on GaAs (001): a static SIMS investigation, J. Phys. Chem. C 114 (12) (2010) 5400–5409.

[11] K. Adlkofer, W. Eck, M. Grunze, M. Tanaka, Surface engineering of Gallium Arsenide with 4-Mercaptobiphenyl monolayers, J. Phys. Chem. B 107 (2003) 587–591.

[12] O. Voznyy, J.J. Dubowski, Structure of Thiol self-assembled monolayers commensurate with the GaAs (001) surface, Langmuir 24 (2008) 13299–13305.

[13] H. Yamamoto, A.R. Butera, Y. Gu, H.D. Waldeck, Characterization of the surface to thiol bonding in self-assembled monolayer films of $C_{12}H_{25}SH$ on InP(100) by angle-resolved X-ray photoelectron spectroscopy, Langmuir 15 (1999) 8640–8644.

[14] P.H. Wampler, Y.D. Zemlyanov, J. Ivanisevic, Comparison between patterns generated by microcontact printing and dip-pen nanolithography on InP surfaces, Phys Chem C Lett. 111 (2007) 17989–17992.

[15] H.H. Park, A. Ivanisevic, Formation and characterization of homogeneous and mixed self-assembled monolayers of peptides and alkanethiols on indium phosphide surfaces, J. Phys. Chem. C 111 (2007) 3710–3718.

[16] W.M. Pruessner, R. Ghodssi, H. Lim, C. Carraro, R. Maboudian, Chemical and thermal stability of alkanethiol and sulfur passivated InP(100), Langmuir 20 (2004) 743–747.

[17] Y. Gu, H.D. Waldeck, Electron tunneling at the semiconductor – insulator – electrolyte interface. photocurrent studies of the n-InP–alkanethiol–ferrocyanide system, J. Phys. Chem. B 102 (1998) 9015–9028.

[18] H. Yamamoto, H.D. Waldeck, Effect of tilt-angle on electron tunneling through organic monolayer films, J. Phys. Chem. B 106 (30) (2002) 7469–7473.

[19] I. Bakish, V. Artel, T. Ilovitsh, M. Shubely, Y. Ben-Ezra, A. Zadok, N.C. Sukenik, Self-assembled monolayer assisted bonding of Si and InP, Opt. Mater. Expr. 2 (8) (2012) 1141–1148.

[20] Y. Xia, X.M. Zhao, G.M. Whitesides, Pattern transfer: self-assembled monolayers as ultrathin resists, Microelectron. Eng. 32 (1996) 255–268.

[21] R.P. Andres, T. Bein, M. Dorogi, S. Feng, J.I. Henderson, C.P. Kubiak, W. Mahoney, R.G. Osifchin, R. Reifenberger, Coulomb staircase" at room temperature in a self--assembled molecular nanostructure, Science 272 (1996) 1323–1325.

[22] H. Hamoudi, V.A. Esaulov, Selfassembly of α,ω-dithiols on surfaces and metal Dithiol heterostructures, Ann. Phys. 528 (2016) 242–263.

[23] J. Käshammer, P. Wohlfart, J. WeiB, C. Winter, R. Fisher, S. Mittler-Neher, Selective gold deposition via CVD onto self-assembled organic monolayers, Opt. Mater. 9 (1998) 406–410.

[24] H. Rieley, K.G. Kendall, W.F. Zemicael, L.T. Smith, S.S. Yang, X-ray studies of self--assembled monolayers on coinage metals. 1. alignment and photooxidation in 1, 8-Octanedithiol and 1-Octanethiol on Au, Langmuir 14 (1998) 5147–5153.

[25] K.A.A. Aliganda, I. Lieberwirth, G. Glasser, S.A. Duwez, Y. Sun, S. Mittler, Fabrication of equally oriented pancake shaped gold nanoparticles by SAM templated OMCVD and their optical response, Org. Electron. 8 (2007) 161–174.

[26] Y. Sakotsubo, T. Ohgi, D. Fujita, Y. Ootuka, Tunneling spectroscopy of isolated gold clusters grown on thiol/dithiol mixed self-assembled monolayers, Phys. E. 29 (2005) 601–605.

[27] J. Liang, G.L. Rosa, G. Scoles, Nanostructuring, Imaging and molecular manipulation of Dithiol monolayers on Au(111) surfaces by atomic force microscopy, J. Phys. Chem. C 111 (2007) 17275–17284.

[28] M. Fahlman, R.W. Salaneck, Surfaces and interfaces in polymer-based electronics, Surf. Sci. 500 (2002) 904–922.

[29] W. Li, L.K.C. Kavanagh, M. Matzke, A.A. Talin, F. Léonard, S. Faleev, W.P.J Hsu, Ballistic electron emission microscopy studies of Au/molecule/n-GaAs diodes, J. Phys. Chem. B 109 (2005) 6252–6256.

[30] W.P.J. Hsu, V.D. Lang, W.K. West, Y. Loo, D.M. Halls, K. Raghavachari, Probing occupied states of the molecular layer in Au–alkanedithiol–GaAs diodes, J. Phys. Chem. B 109 (2005) 5719–5723.

[31] H. Hamoudi, K. Uosaki, K. Ariga, V.A. Esaulov, Going beyond the self-assembled monolayer: metal intercalated dithiol multilayers and their conductance, RSC Adv. 4 (2014) 39657–39666.

[32] H. Hamoudi, Crossbar nanoarchitectonics of the crosslinked self-assembled monolayer, Nanoscale Res. Lett. 9 (2014) 287.

[33] S. Pethkar, M. Aslam, S.I. Mulla, P. Ganeshan, K. Vijayamohanan, Preparation and characterisation of silver quantum dot superlattice using self-assembled monolayers of pentanedithiol, J. Mater. Chem. 11 (2001) 1710–1714.

[34] V.K. Sarathy, J.P. Thomas, U.G. Kulkarni, N.R.C. Rao, Superlattices of metal and metal–semiconductor quantum dots obtained by layer-by-layer deposition of nanoparticle arrays, J. Phys. Chem. B 103 (1999) 399–401.

[35] H. Hamoudi, Bottom-up nanoarchitectonics of two-dimensional freestanding metal doped carbon nanosheet, RSC Adv. 4 (2014) 22035–22041.

[36] H. Hamoudi, Carbon–metal nanosheets from the water–hexane interface, J. Mater. Chem. C 3 (2015) 3636–3644.

[37] F. Schreiber, Structure and growth of self-assembling monolayers, Prog. Surf. Sci. 65 (2000) 151–257.

[38] C. Vericat, M.E. Vela, A.G. Benitez, A.M.J. Gago, X. Torrelles, R.C. Salvarezza, Surface characterization of sulfur and alkanethiol self-assembled monolayers on Au(111), J. Phys. 18 (2006) R867-R900.

[39] P. Maksymovych, O. Voznyy, B.D. Dougherty, C.D. Sorescu, T.J. Yates Jr, Gold adatom as a key structural component in self-assembled monolayers of organosulfur molecules on Au(111), Surf. Sci. 85 (2009) 206–240.

[40] G.R. Nuzzo, A.F. Fusco, L.D. Allara, Spontaneously organized molecular assemblies. 3. preparation and properties of solution adsorbed monolayers of organic disulfides on gold surfaces, J. Am. Chem. Soc. 109 (8) (1987) 2358–2368.

[41] E. Sabatani, C.J. Boulakia, M. Bruening, I. Rubinstein, Thioaromatic monolayers on gold: a new family of self-assembling monolayers, Langmuir 9 (1993) 2974–2981.

[42] D.M. Porter, B.T. Bright, L.D. Allara, E.D.C. Chidsey, Spontaneously organized molecular assemblies. 4. structural characterization of n-alkyl thiol monolayers on gold by optical ellipsometry, infrared spectroscopy, and electrochemistry, J. Am. Chem. Soc. 109 (1987) 3559–3568.

[43] G.D Castner, K. Hinds, W.D. Grainger, Photoelectron spectroscopy sulfur 2p study of organic Thiol and disulfide binding interactions with gold surfaces, Langmuir 12 (1996) 5083–5086.

[44] E. Ito, H. Kang, D. Lee, J.B. Park, M. Hara, J. Noh, Spontaneous desorption and phase transitions of self-assembled Alkanethiol and Alicyclic Thiol monolayers chemisorbed on Au(111) in ultrahigh vacuum at room temperature, J. Colloid Interface Sci. 394 (2013) 522–529.

[45] M. Prato, R. Moroni, F. Bisio, R. Rolandi, L. Mattera, O. Cavalleri, M. Canepa, Optical characterization of thiolate self-assembled monolayers on Au(111), J. Phys. Chem. C 112 (2008) 3899–3906.

[46] Z. Guo, W. Zheng, H. Hamoudi, C. Dablemont, V.A. Esaulov, B. Bourguignon, On the chain length dependence of CH3 vibrational mode relative intensities in sum frequency generation spectra of self-assembled alkanethiols, Surf. Sci. 602 (2008) 3551–3559.

[47] D.C. Bain, B.E. Troughton, T.Y. Tao, J. Evall, M.G. Whitesides, G.R. Nuzzo, Formation of monolayer films by the spontaneous assembly of organic thiols from solution onto gold, J. Am. Chem. Soc. 111 (1) (1989) 321–335.

[48] M.J. Tour, L. Jones, D. Pearson, J. Lamba, T. Burgin, M.G. Whitesides, L.D. Allara, N.A. Parikh, V.S. Atre, Self-assembled monolayers and multilayers of conjugated thiols, alpha.omega.-dithiols, and thioacetyl-containing adsorbates. understanding attachments between potential molecular wires and gold surfaces, J. Am. Chem. Soc. 117 (37) (1995) 9529–9534.

[49] B. De Boer, H. Meng, F.D. Perepichka, J. Zheng, M.M. Frank, J.Y. Chabal, Z. Bao, Synthesis and characterization of conjugated Mono- and Dithiol oligomers and characterization of their self-assembled monolayers, Langmuir 19 (10) (2003) 4272–4284.

[50] P. Kohli, K.K. Taylor, J.J. Harris, J.G. Blanchard, Assembly of covalently-coupled disulfide multilayers on gold, J. Am. Chem. Soc. 120 (1998) 11962–11968.

[51] S. Rifai, M. Morin, Isomeric effect on the oxidative formation of bilayers of benzenedimethanethiol on Au(111), J. Electroanal. Chem. 550– 551 (2003) 277–289.

[52] H. Hamoudi, Z.A. Guo, M. Prato, C. Dablemont, W.Q. Zheng, B. Bourguignon, M. Canepa, V.A. Esaulov, On the self-assembly of short chain alkanedithiols, Phys. Chem. Chem. Phys. 10 (2008) 6836–6841.

[53] H. Hamoudi, M. Prato, C. Dablemont, O. Cavalleri, M. Canepa, V.A. Esaulov, Self--Assembly of 1,4-benzenedimethanethiol self-assembled monolayers on gold, Langmuir 26 (2010) 7242–7247.

[54] L. Pasquali, F. Terzi, R. Seeber, S. Nannarone, D. Datta, C. Dablemont, H. Hamoudi, M. Canepa, V.A. Esaulov, UPS, XPS, and NEXAFS study of self-assembly of standing 1,4-benzenedimethanethiol SAMs on gold, Langmuir 27 (2011) 4713–4720.

[55] J. Jia, S. Mukherjee, H. Hamoudi, S. Nannarone, L. Pasquali, V. Esaulov, Lying-Down to standing-up transitions in self assembly of Butanedithiol monolayers on gold and substitutional assembly by octanethioles, J. Phys. Chem. C 117 (2013) 4625–4631.

[56] K. Kitagawa, T. Morita, S. Kimura, Electron transport properties of helical peptide dithiol at a molecular level: scanning tunneling microscope study, Thin Solid Films 509 (2006) 18–26.

[57] P.F. Cometto, G. Ruano, H. Ascolani, G.E. Zampieri, Adlayers of alkanedithiols on Au(111): effect of disulfide reducing agent, Langmuir 29 (5) (2013) 1400–1406.

[58] W.P.J. Hsu, L.Y Loo, V.D. Lang, A.J. Rogers, Nature of electrical contacts in a metal–molecule–semiconductor system, J. Vac. Sci. Technol. B 21 (2003) 1928.

[59] N.A. Caruso, R. Rajesh, G. Gallup, J. Redepenning, A.P. Dowben, Orientation and bonding of biphenyldimethyldithiol, J. Phys: Condens Matter 16 (6) (2004) 845–860.
[60] L. Pasquali, F. Terzi, C. Zanardi, R. Seeber, G. Paolicelli, N. Mahne, S. Nannarone, Bonding and orientation of 1,4-benzenedimethanethiol on Au(111) prepared from solution and from gas phase J, Phys 19 (2007) 305020.
[61] L. Pasquali, F. Terzi, R. Seeber, B.P. Doyle, S. Nannarone, Adsorption geometry variation of 1,4-benzenedimethanethiol self-assembled monolayers on Au(111) grown from the vapor phase, J. Chem. Phys. 128 (13) (2008) 134711.
[62] L. Salazar Alarcón, J.L. Cristina, J. Shen, J. Jia, A.V. Esaulov, E.A. Sánchez, O. Grizzi, Growth of 1,4-benzenedimethanethiol films on Au, Ag, and Cu: effect of surface temperature on the adsorption kineticas and on the single versus multilayer formation, J. Phys. Chem. C 117 (34) (2013) 17521–17530.
[63] J. Jia, J. Kara, L. Pasquali, A. Bendounan, F. Sirotti, V.A. Esaulov, On sulfur core level binding energies in thiol self-assembly and alternative adsorption sites:an experimental and theoretical study, J. Chem. Phys. 143 (2015) 104702.
[64] L. Rodríguez, E.J. Gayone, A.E. Sánchez, H. Ascolani, O. Grizzi, M. Sánchez, B. Blum, G. Benitez, R. Salvarezza, Adsorption of short-chain alkanethiols on Ag(111) studied by direct recoiling spectroscopy, Surf. Sci. 600 (2006) 2305–2316.
[65] S. Nannarone, F. Borgatti, A. De Luisa, B.P. Doyle, G.C. Gazzadi, A. Giglia, P. Finetti, N. Mahne, L. Pasquali, M. Pedio, G. Selvaggi, G. Naletto, M.G. Pelizzo, G. Tondello, The BEAR beamline at elettra, AIP Conf. Proc. 705 (2004) 450–453.
[66] J.W. Rabalais, Principles and applicatiopns of ion scattering spectrometry, Wiley –Interscience Series on Mass Spectroscopy, 2003 ISBN 0-471-20277-0.
[67] M.W. Lau, N.S.R. Sodhi, J.B. Flinn, H.K. Tan, M.G. Bancroft, Photoemission study of sputter-etched InP surfaces, Appl. Phys. Lett. 51 (3) (1987) 177–179.
[68] T. Kendelewicz, H.P. Mahowald, A.K. Bertness, E.C. McCants, I. Lindau, E.W. Spicer, Surface shifts in the In 4d and P 2p core-level spectra of InP(110), Phys. Rev. B 36 (1987) 6543–6546.
[69] A. McKinley, W.A. Parke, H.R. Willias, Silver Overlayers on (110) Indium Phosphide:film growth and Schottky barrier formation, J. Phys. C 13 (1980) 6723–6736.
[70] E.J. Gayone, G.R. Pregliasco, E.A. Sánchez, O. Grizzi, Topographic and crystallographic characterization of a grazing ion bombarded GaAs (110) surface by TOF-ISS, Phys. Rev. B. 56 (1997) 4186–4193.
[71] J. Jia, A. Giglia, M. Flores, O. Grizzi, L. Pasquali, V.A. Esaulov, 1,4-Benzenedimethanethiol interaction with Au(110), Ag(111), Cu(100), and Cu(111) surfaces: self-assembly and dissociation processes, J. Phys. Chem. C 118 (2014) 26866–26876.
[72] A. Shaporenko, K. Adlkofer, L.S.O. Johansson, M. Tanaka, M. Zharnikov, Functionalization of GaAs surfaces with aromatic self-assembled monolayers: a synchrotron-based spectroscopic study, Langmuir 19 (12) (2003) 4992–4998.
[73] H. Hamoudi, F. Chesneau, C. Patze, M. Zharnikov, Chain-length-dependent branching of irradiation-induced processes in alkanethiolate self-assembled monolayers, J. Phys. Chem. C 115 (2) (2011) 534–541.
[74] D. Zerulla, T. Chasse, X-ray induced damage of self-assembled alkanethiols on gold and indium phosphide, Langmuir 15 (16) (1999) 5285–5294.
[75] D. Fracasso, D. Kumar, P. Rudolf, R.C. Chiechi, Self-assembled monolayers of terminal acetylenes as replacements for thiols in bottom-up tunneling junctions, RSC Adv. 4 (2014) 56026–56030.
[76] S. Zhang, K.L. Chandra, C.B. Gorman, Self-assembled monolayers of terminal alkynes on gold, J. Am. Chem. Soc. 129 (2007) 4876–4877.